

DMFORMER: CLOSING THE GAP BETWEEN CNN AND VISION TRANSFORMERS

Zimian Wei¹, Hengyue Pan¹, Lujun Li², Menglong Lu¹, Xin Niu¹, Peijie Dong¹, Dongsheng Li¹

¹ College of Computer, National University of Defense Technology

² Chinese Academy of Sciences, Beijing, China

ABSTRACT

Vision transformers have shown excellent performance in computer vision tasks. As the computation cost of their self-attention mechanism is expensive, recent works tried to replace the self-attention mechanism in vision transformers with convolutional operations, which is more efficient with built-in inductive bias. However, these efforts either ignore multi-level features or lack dynamic prosperity, leading to sub-optimal performance. In this paper, we propose a Dynamic Multi-level Attention mechanism (DMA), which captures different patterns of input images by multiple kernel sizes and enables input-adaptive weights with a gating mechanism. Based on DMA, we present an efficient backbone network named DMFormer. DMFormer adopts the overall architecture of vision transformers, while replacing the self-attention mechanism with our proposed DMA. Extensive experimental results on ImageNet-1K and ADE20K datasets demonstrated that DMFormer achieves state-of-the-art performance, which outperforms similar-sized vision transformers (ViTs) and convolutional neural networks (CNNs).

Index Terms— vision transformer; CNN; attention mechanism; multi-level feature

1. INTRODUCTION

Recently, vision transformers (ViT) [1, 2] have drawn growing attention in computer vision research. Due to the capacity of modeling long-range dependencies, ViTs are specialized in extracting global features. However, the self-attention mechanism in transformers brings about heavy computation costs, making them unaffordable for high-resolution downstream tasks (e.g., semantic segmentation). Although recent local vision transformer methods [3, 4] alleviate this problem to some extent, the implementation of cross-window strategies in local self-attention is still sophisticated.

As a complementary, convolution neural network (CNN) focus on capturing local relations with high efficiency. With built-in inductive biases, CNNs are easy to train with quick convergence. To this end, there is a trend to take the merits of both CNNs and ViTs by migrating desired properties of ViTs to CNNs, including the overall architecture design, large receptive field, and data specificity provided by the at-

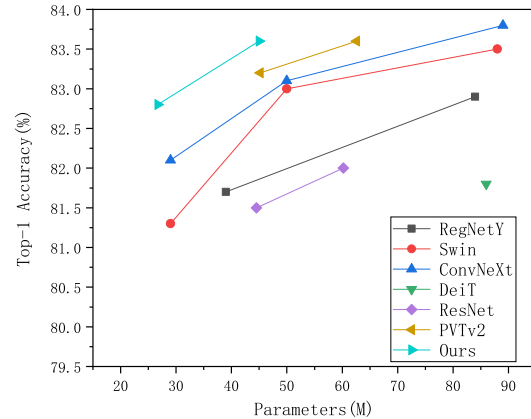


Fig. 1. Results of different models on ImageNet-1K validation set. We compare accuracy-parameters trade-off of recent models RegNet [9], Swin Transformer [3], ConvNeXt [5], DeiT [2], ResNet [6], PVTv2 [10] and our DMFormer.

Table 1. Favorable properties correspond to different modules, including self-attention, multi-scale convolution, dilated convolution, and DMA.

Properties	Self-attention	Multi-scale Convolution	Dilated Convolution	DMA
Local inductive bias	✗	✓	✓	✓
Large receptive field	✓	✗	✓	✓
Multi-scale Interaction	✗	✓	✓	✓
Input Adaptive	✓	✗	✗	✓

tention mechanism. For example, ConvNext [5] built a pure CNN family based on ResNet [6], which performs on par or slightly better than ViT by learning their training procedure and macro/micro-level architecture designs. RepLKNet [7] adopts as large as 31×31 kernel size to enlarge effective receptive fields following the design in ViT. Although encouraging performance has been achieved by the above methods, their computation costs are relatively large. [8] competes favorably with Swin transformer [3] by replacing the local self-attention layer with the dynamic depth-wise convolution layer, while keeping the overall structure unchanged. However, the lack of multi-level features limits its capacity to achieve better performance.

In this paper, we propose a new dynamic multi-level at-

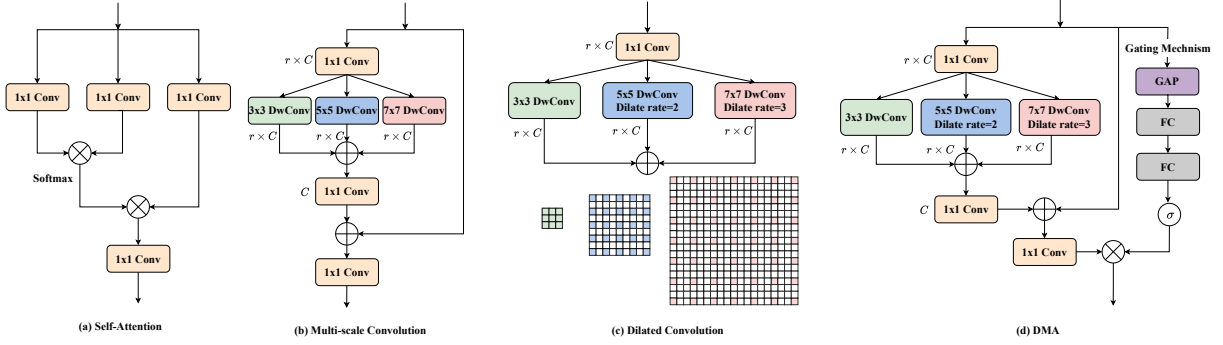


Fig. 2. The structure comparison between related modules: self-attention (a), multi-scale convolution (b), dilated convolution (c), and DMA (d). DwConv, GAP, σ , and FC refer to depth-wise convolution, global average pool, sigmoid function, and fully connected layer, respectively. C refers to the number of channels, while r is the expansion ratio in the DMA.

tention (DMA) mechanism (see Table 1 and Fig. 2 for more details). Firstly, DMA is characterized by applying multiple kernel sizes for different resolution patterns. As mentioned in [11], multiple kernel sizes can effectively improve the model’s performance. Secondly, DMA involves dilated convolutions to efficiently enlarge the receptive field. Thirdly, we design a lightweight gating mechanism in DMA to provide input adaptability, with which the channel-wise relationships are captured and the representational power of the network is enhanced. Based on DMA, we extend the architecture of Swin Transformer [3] and propose a new framework named DMFormer. The experimental results show that DMFormer achieves state-of-the-art performance on ImageNet classification (see Fig. 1) and semantic segmentation tasks.

In summary, the contributions of this paper have two aspects: 1) We propose a new attention mechanism named DMA, which combines the advantages of convolution and self-attention. 2) Based on DMA, we design a backbone model named DMFormer. Extensive experiments on ImageNet classification and semantic segmentation tasks show the superior of DMFormer over other existing models.

2. APPROACHES

In this section, we first present details of DMA. Then we show the overall structure and present different architecture designs in DMFormer family.

2.1. DMA

We illustrate the structure of DMA in Fig. 2 (d). The two key components in DMA are the multi-scale dilated convolution and gating mechanism. Multi-scale dilated convolution captures different patterns with various resolutions of input images, while the gating mechanism learns to selectively emphasize informative features by re-calibration.

Assuming that the input of DMA is X . As depicted in Fig. 2 (d), a 1×1 convolution layer ($Conv_{\text{exp},r} 1 \times 1$) is applied to expand the number of channels by r times. Then, a

parallel design of 3×3 , 5×5 , 7×7 depth-wise convolution is introduced to learn multi-scale features. BatchNorm and ReLU are followed to prevent over-fit when training. Next, in order to apply a residual connection for better optimization, we apply a 1×1 convolution layer to reduce the number of channels as the original input X . The above operators can be expressed as follows:

$$\begin{aligned} X_E &= Conv_{\text{exp},r} 1 \times 1 (X), \\ X_1, X_2, X_3 &= Parallel_{3 \times 3, 5 \times 5, 7 \times 7} (X_E), \\ X_P &= \text{ReLU} (BN (X_1 + X_2 + X_3)), \\ X' &= X + Conv 1 \times 1 (X_P), \end{aligned} \quad (1)$$

where $Parallel_{3 \times 3, 5 \times 5, 7 \times 7}$ contains multi-branch of 3×3 , 5×5 , 7×7 convolution layers. Specifically, for branches with kernel size 5×5 and 7×7 , we set the corresponding dilated rates as 2, 3 to obtain larger receptive field.

For the gating mechanism, we apply a global average pooling (GAP) layer to obtain global information, followed by two successive fully connected layers. At last, a sigmoid function is applied to compute the attention vector. The operations in the gating mechanism can be formulated as follows:

$$\begin{aligned} V &= \text{ReLU} (FC (GAP (X))), \\ \text{Attn} &= \text{Sigmoid} (FC (V)), \end{aligned} \quad (2)$$

Finally, the output of DMA is obtained by re-calibrating the fused feature X' with the gating mechanism as follows:

$$\text{Output} = \text{Attn} \otimes Conv 1 \times 1 (X'), \quad (3)$$

where \otimes means the element-wise matrix multiplication.

In the following section, we will introduce the basic block, overall framework, and detailed architectural design in DMFormer family.

2.2. DMFormer

We build DMFormer with a hierarchical design similar to traditional CNNs [6] and recent local vision transformers [3].

Table 2. The detailed setting for different versions of DMFormer. ER, r represent the expansion ratio in the MLP module and DMA module, respectively.

stage	output size	ER	r	DMFormer-S	DMFormer-L
1	$\frac{H}{4} \times \frac{W}{4} \times C_1$	8	4	$C_1 = 64$ $N_1 = 2$	$C_1 = 64$ $N_1 = 3$
2	$\frac{H}{8} \times \frac{W}{8} \times C_2$	8	4	$C_2 = 128$ $N_2 = 2$	$C_2 = 128$ $N_2 = 3$
3	$\frac{H}{16} \times \frac{W}{16} \times C_3$	4	4	$C_3 = 320$ $N_3 = 6$	$C_3 = 320$ $N_3 = 12$
4	$\frac{H}{32} \times \frac{W}{32} \times C_4$	4	4	$C_4 = 512$ $N_4 = 2$	$C_4 = 512$ $N_4 = 3$
Parameters (M)				26.7	45.0
FLOPs (G)				5.0	8.7

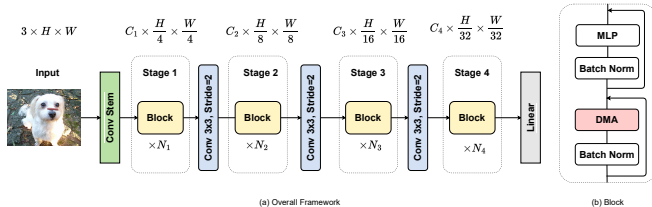


Fig. 3. (a) The overall framework of DMFormer. Following [3], DMFormer adopts the hierarchical architecture with 4 stages, and each stage consists of multiple blocks. C_i, N_i refer to the feature dimension and block number in stage i , respectively. (b) The basic block in DMFormer. We apply the modular design in vision transformers, while replacing the self-attention layer with DMA.

Fig. 3 (a) presents the overall framework of DMFormer and Fig. 3 (b) shows the basic block in DMFormer.

The input image I is first processed by the convolution stem module, which consists of a 7×7 convolution layer with a stride of 2, a 3×3 convolution layer with a stride of 1, and a non-overlapping 2×2 convolution layer with a stride of 2. Then the spatial size of output features after the convolution stem module is $\frac{H}{4} \times \frac{W}{4}$.

$$X = \text{ConvStem}(I), \quad (4)$$

where $X \in \mathbb{R}^{N \times C_1 \times \frac{H}{4} \times \frac{W}{4}}$ is the output feature of the convolution stem module. N, C_1 is the batch size and number of channels. Then X is fed to repeated DMFormer blocks, each of which consists of two sub-blocks. Specifically, the main components of the first sub-block include DMA and the BatchNorm module, which we present as

$$Y = \text{DMA}(\text{BN}(X)) + X, \quad (5)$$

where $\text{BN}(\cdot)$ denotes a Batch Normalization. Details of $\text{DMA}(\cdot)$ are depicted in Section 2.1. The second sub-block consists of two fully-connected layers and a non-linear activation GELU [12]. The output of the MLP module is formulated as follows:

$$Z = \text{GELU}(W_1(\text{BN}(Y))W_2 + Y), \quad (6)$$

Table 3. Compare with the state-of-the-art methods on the ImageNet validation set. Params means parameter. GFLOPs donates floating point operations.

Method	Params. (M)	GFLOPs	Top-1 Acc (%)
PVT-Small [18]	24.5	3.8	79.8
Swin-T [3]	28.3	4.5	81.3
PoolFormer-S36 [19]	31.0	5.2	81.4
Twins-SVT-S [20]	24.0	2.8	81.7
Focal-T [14]	29.1	4.9	82.2
ConvNeXt-T [5]	28.6	4.5	82.1
DMFormer-S	26.7	5.0	82.8
PVT-Medium [18]	44.2	6.7	81.2
Focal-S [14]	51.1	9.1	83.5
Swin-S [3]	49.6	8.7	83.0
ConvNeXt-S [5]	50.0	8.7	83.1
DMFormer-L	45.0	8.7	83.6

where $W_1 \in \mathbb{R}^{C_i \times eC_i}$ and $W_2 \in \mathbb{R}^{eC_i \times C_i}$ are learnable parameters in fully connected layers. e is the MLP expansion ratio for the number of channels; C_i is the number of channels in the corresponding stage.

Based on the above DMFormer block, we formulate DMFormer-S and DMFormer-L with different model sizes. The numbers of channels corresponding to the four stages are identical for both DMFormer-S and DMFormer-L, which are set as 64, 128, 320, and 512. Differently, DMFormer-L is larger with more block numbers. Specifically, stages 1, 2, 3, and 4 of DMFormer-S contain 2, 2, 6, 2 blocks, while that for DMFormer-L are 3, 3, 12, 3, respectively. Their detailed architecture designs are shown in Table 2.

3. EXPERIMENTS

3.1. Image classification

We conduct image classification experiments on ImageNet-1K [13]. Each model is trained for 300 epochs with AdamW optimizer, and a total batch size of 1024 on 8 GPUs. The initial learning rate is set as $1e-3$. We adopt the cosine decay schedule to adjust the learning rate during training.

Table 3 summarizes the experimental results on ImageNet-1K classification. Comparing with recently well-established ViTs like Swin-S [3] and Focal-S [14], DMFormer consistently shows better performance. Specifically, DMFormer-L surpasses Swin-S, Focal-S by 0.6%, 0.1% top-1 accuracy with 9%, 12% fewer parameters. Comparatively, ConvNeXt [5] is an excellent CNN that learns architecture designs and training schedules from ViTs for better performance. DMFormer-L outperforms ConvNeXt-S by 0.5%, while reducing the model size by 10%. Moreover, in Fig. 4 (a), we utilize Grad-CAM [15] to localize discriminative regions generated by Swin-T [16], ResNet50 [6] and DMFormer-S. It can be observed that the highlighted class activation area of DMFormer-S is more accurate. The experimental results demonstrate the superiority of DMFormer.

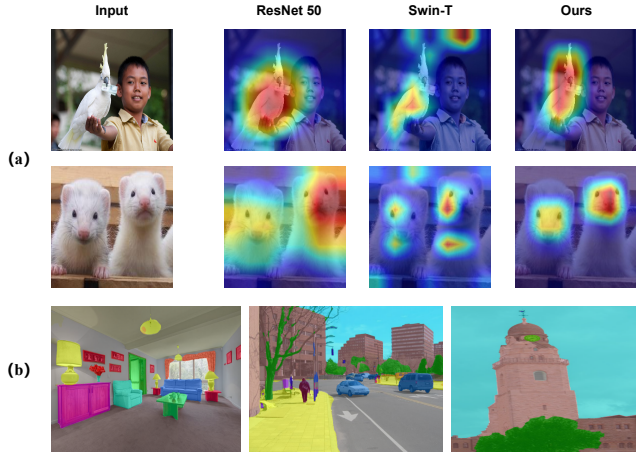


Fig. 4. (a) Grad-CAM [15] results generated by Swin-T [3], ResNet50 [6] and ours. The images are randomly selected from the ImageNet validation dataset. Lighter colors in Grad-CAM results refer to stronger attention regions. (b) Visualization results of semantic segmentation on ADE20K [17] with ImageNet pre-trained DMFormer-S as the backbone.

3.2. Semantic segmentation

We evaluate models for the semantic segmentation task on ADE20K [17]. mIoU (mean Intersection Over Union) is applied to measure the model performance. Semantic FPN [21] and UperNet [22] are used as main frameworks to evaluate the DMFormer-S backbone. Pre-trained weights on ImageNet-1K are utilized to initialize our backbone. We train each model with AdamW optimizer, a total batch size of 16 on 8 GPUs. When equipped with Semantic FPN [21], we use the 40K-iteration training scheme in [18, 19]. The learning rate is set as 2×10^{-4} and decays by polynomial schedule with a power of 0.9. Comparatively, we adopt the 160K-iteration training scheme in [3] for UperNet. Specifically, the learning rate is set as 6×10^{-5} with 1500 iteration warmup and linear learning rate decay.

Table 4 lists the performance of different backbones using FPN and UperNet. Generally, DMFormer consistently outperforms other state-of-the-art backbones. When using Semantic FPN for semantic segmentation, DMFormer-S surpasses VAN-B2 [24] by 0.5 mIoU with similar computation cost. Moreover, although the parameter of DMFormer-S is 37% smaller than that of PVT-Medium [18], the mIoU is still 5.6 points higher (47.2 vs 41.6). When applying UperNet as the framework, our model outperforms ConvNeXt-T [5] by 0.9 mIoU, with about 6% model size reduction. Additionally, DMFormer-S is 1.8 mIoU higher than Focal-T [14] with 9% decreased parameters. In Fig. 4 (b), we present visualization of semantic segmentation results applying UperNet [22]. The results indicate the powerful capacity of DMFormer for the semantic segmentation task.

Table 4. Results of semantic segmentation on ADE20K [17] validation set. The pre-trained DMFormer-S is applied as the backbone and plugged in Semantic FPN [21] and UperNet [22] frameworks. Note that the difference in the number of parameters between two DMFormer-S is due to the usage of semantic FPN and UperNet.

Method	Backbone	#Param (M)	mIoU (%)
Semantic FPN [21]	ResNet101 [6]	47.5	38.8
	ResNeXt101-32x4d [23]	47.1	39.7
	PoolFormer-S36 [19]	34.6	42.0
	PVT-Medium [18]	48.0	41.6
	TwinP-S [20]	28.4	44.3
	VAN-B2 [24]	30.0	46.7
	DMFormer-S	30.4	47.2
UperNet [22]	ConvNeXt-T [5]	60.0	46.7
	Swin-T [3]	60.0	46.1
	TwinP-S [20]	54.6	46.2
	Focal-T [14]	62.0	45.8
	DMFormer-S	56.6	47.6

Table 5. Ablation study of different modules in DMA. Block numbers are modified to achieve comparable computation complexity. We adopt Semantic FPN [21] as main framework, and use ImageNet pre-trained DMFormer-S variants as backbone for semantic segmentation. Parameters and FLOPs are calculated under the ImageNet classification setting.

Variants	Blocks	Params. (M)	FLOPs (G)	ImageNet Top-1 Acc	ADE20k mIoU
w/o Expansion rate r	2, 2, 12, 2	26.9	5.0	82.8	46.3
w/o Multi-scale Conv	2, 2, 6, 2	26.2	4.9	82.5	46.0
w/o Dilation	2, 2, 6, 2	26.7	5.0	82.4	46.4
w/o Gating Mechanism	2, 2, 7, 2	26.2	5.4	82.7	45.7
DMFormer-S	2, 2, 6, 2	26.7	5.0	82.8	47.2

3.3. Ablation studies

We conduct ablation studies on each component of DMA module to shed light on various architecture designs. DMFormer-S is adopted as the baseline model. In the w/o multi-scale Conv variant, we only keep a single convolution branch with 7×7 kernel size. For w/o Expansion rate variant, we set r in the DMA (see Table 2 and Fig. 2) as 1. To achieve comparable model complexity, we modify block numbers in some variants. The experimental results in Table 5 indicate that all components in DMA are non-trivial to improve performance.

4. CONCLUSION

In this paper, we have introduced DMFormer, a novel efficient vision backbone that outperforms most similar-sized state-of-the-art models on ImageNet classification and semantic segmentation tasks. We have also presented DMA, the key component of DMFormer which shows much efficiency over the existing self-attention mechanisms. Future work may include adapting DMFormer to other tasks such as video processing and object detection, or extending DMA to a hybrid design with existing excellent CNN or self-attention mechanisms to further enhance performance.

5. REFERENCES

- [1] Alexey Dosovitskiy, Lucas Beyer, Alexander Kolesnikov, and Dirk Weissenborn, “An image is worth 16x16 words: Transformers for image recognition at scale,” in *International Conference on Learning Representations*, 2020.
- [2] Hugo Touvron, Matthieu Cord, Alexandre Sablayrolles, and Hervé Jégou, “Training data-efficient image transformers & distillation through attention,” in *International Conference on Machine Learning*. PMLR, 2021, pp. 10347–10357.
- [3] Ze Liu, Yutong Lin, Yue Cao, and Baining Guo, “Swin transformer: Hierarchical vision transformer using shifted windows,” in *Proceedings of the IEEE/CVF International Conference on Computer Vision (ICCV)*, October 2021, pp. 10012–10022.
- [4] Zilong Huang, Youcheng Ben, Guozhong Luo, Pei Cheng, Gang Yu, and Bin Fu, “Shuffle transformer: Rethinking spatial shuffle for vision transformer,” *arXiv preprint arXiv:2106.03650*, 2021.
- [5] Zhuang Liu, Hanzi Mao, Chao-Yuan Wu, Christoph Feichtenhofer, Trevor Darrell, and Saining Xie, “A convnet for the 2020s,” *arXiv preprint arXiv:2201.03545*, 2022.
- [6] Kaiming He, Xiangyu Zhang, Shaoqing Ren, and Jian Sun, “Deep residual learning for image recognition,” in *CVPR*, 2016, pp. 770–778.
- [7] Xiaohan Ding, Xiangyu Zhang, Jungong Han, and Guiguang Ding, “Scaling up your kernels to 31x31: Revisiting large kernel design in cnns,” in *CVPR*, 2022, pp. 11963–11975.
- [8] Qi Han, Zejian Fan, Qi Dai, Lei Sun, Ming-Ming Cheng, Jiaying Liu, and Jingdong Wang, “On the connection between local attention and dynamic depth-wise convolution,” in *International Conference on Learning Representations*, 2021.
- [9] Ilija Radosavovic, Raj Prateek Kosaraju, Ross Girshick, Kaiming He, and Piotr Dollár, “Designing network design spaces,” 2020, pp. 10428–10436.
- [10] Wenhai Wang, Enze Xie, Tong Lu, Ping Luo, and Ling Shao, “Pvtv2: Improved baselines with pyramid vision transformer,” *arXiv preprint arXiv:2106.13797*, 2021.
- [11] Mingxing Tan and Quoc V Le, “Mixconv: Mixed depthwise convolutional kernels,” *arXiv preprint arXiv:1907.09595*, 2019.
- [12] Dan Hendrycks and Kevin Gimpel, “Gaussian error linear units (gelus),” *arXiv preprint arXiv:1606.08415*, 2016.
- [13] Jia Deng, Wei Dong, Richard Socher, Li-Jia Li, Kai Li, and Li Fei-Fei, “Imagenet: A large-scale hierarchical image database,” in *2009 IEEE conference on computer vision and pattern recognition*. Ieee, 2009, pp. 248–255.
- [14] Jianwei Yang, Chunyuan Li, Pengchuan Zhang, Xiyang Dai, Bin Xiao, Lu Yuan, and Jianfeng Gao, “Focal self-attention for local-global interactions in vision transformers,” *arXiv preprint arXiv:2107.00641*, 2021.
- [15] Ramprasaath R Selvaraju, Michael Cogswell, Abhishek Das, Ramakrishna Vedantam, Devi Parikh, and Dhruv Batra, “Grad-cam: Visual explanations from deep networks via gradient-based localization,” 2017, pp. 618–626.
- [16] Ze Liu, Yutong Lin, Yue Cao, Stephen Lin, and Baining Guo, “Swin transformer: Hierarchical vision transformer using shifted windows,” 2021.
- [17] Bolei Zhou, Hang Zhao, and Antonio Torralba, “Scene parsing through ade20k dataset,” in *CVPR*, 2017, pp. 633–641.
- [18] Wenhai Wang, Enze Xie, Ping Song, and Ling Shao, “Pyramid vision transformer: A versatile backbone for dense prediction without convolutions,” in *ICCV*, October 2021, pp. 568–578.
- [19] Weihao Yu, Mi Luo, and Shuicheng Yan, “Metaformer is actually what you need for vision,” in *CVPR*, 2022, pp. 10819–10829.
- [20] Xiangxiang Chu, Zhi Tian, Yuqing Wang, Bo Zhang, Haibing Ren, Xiaolin Wei, Huaxia Xia, and Chunhua Shen, “Twins: Revisiting the design of spatial attention in vision transformers,” vol. 34, 2021.
- [21] Alexander Kirillov, Ross Girshick, Kaiming He, and Piotr Dollár, “Panoptic feature pyramid networks,” 2019, pp. 6399–6408.
- [22] Tete Xiao, Yingcheng Liu, Bolei Zhou, Yuning Jiang, and Jian Sun, “Unified perceptual parsing for scene understanding,” 2018, pp. 418–434.
- [23] Saining Xie, Ross Girshick, Piotr Dollár, Zhuowen Tu, and Kaiming He, “Aggregated residual transformations for deep neural networks,” in *CVPR*, 2017, pp. 1492–1500.
- [24] Meng-Hao Guo, Cheng-Ze Lu, Zheng-Ning Liu, Ming-Ming Cheng, and Shi-Min Hu, “Visual attention network,” *arXiv preprint arXiv:2202.09741*, 2022.